HHS Public Access

Author manuscript

ACS Biomater Sci Eng. Author manuscript; available in PMC 2018 May 07.

Published in final edited form as:

ACS Biomater Sci Eng. 2017 March 13; 3(3): 420–430. doi:10.1021/acsbiomaterials.6b00805.

Chondroitin Sulfate Glycosaminoglycan Matrices Promote Neural Stem Cell Maintenance and Neuroprotection Post-Traumatic Brain Injury

Martha I. Betancur[†], **Hannah D. Mason**[†], **Melissa Alvarado-Velez**[§], **Phillip V. Holmes**[‡], **Ravi V. Bellamkonda**[§], and **Lohitash Karumbaiah**[*,†]

[†]Regenerative Bioscience Center, The University of Georgia, 425 River Road, ADS Complex, Athens, Georgia 30602, United States

[‡]Psychology Department, The University of Georgia, 125 Baldwin Street, Athens, Georgia 30602, United States

[§]Wallace H. Coulter Department of Biomedical Engineering, Georgia Institute of Technology, 313 Ferst Drive, Atlanta, Georgia 30332, United States

Abstract

There are currently no effective treatments for moderate-to-severe traumatic brain injuries (TBIs). The paracrine functions of undifferentiated neural stem cells (NSCs) are believed to play a significant role in stimulating the repair and regeneration of injured brain tissue. We therefore hypothesized that fibroblast growth factor (FGF2) enriching chondroitin sulfate glycosaminoglycan (CS-GAG) matrices can maintain the undifferentiated state of neural stem cells (NSCs) and facilitate brain tissue repair subacutely post-TBI. Rats subjected to a controlled cortical impactor (CCI) induced TBI were intraparenchymally injected with CS-GAG matrices alone or with CS-GAG matrices containing PKH26GL labeled allogeneic NSCs. Nissl staining of brain tissue 4 weeks post-TBI demonstrated the significantly enhanced ($p < 0.05$) tissue protection in CS-GAG treated animals when compared to TBI only control, and NSC only treated animals. CS-GAG-NSC treated animals demonstrated significantly enhanced ($p < 0.05$) FGF2 retention, and maintenance of PKH26GL labeled NSCs as indicated by enhanced Sox1+ and Ki67+ cell presence over other differentiated cell types. Lastly, all treatment groups and sham controls exhibited a significantly ($p < 0.05$) attenuated GFAP+ reactive astrocyte presence in the lesion site when compared to TBI only controls.

Graphical Abstract

[*]Corresponding Author: lohitash@uga.edu. Tel: (706) 542-2017. Fax: (706) 583-0274.

ORCID

Lohitash Karumbaiah: 0000-0001-7969-417X

Notes

The authors declare no competing financial interest.

Supporting Information

The Supporting Information is available free of charge on the ACS Publications website at DOI: 10.1021/acsbiomater-ials.6b00805.

Figures S1–S4 (PDF)

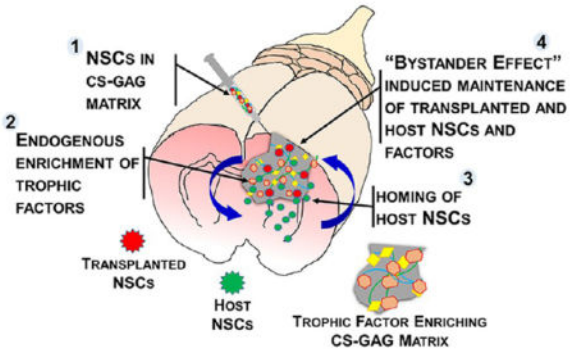

Keywords

traumatic brain injury; biomaterials; neuroprotection; chondroitin sulfate glycosaminoglycan; neural stem cells; hydrogels

1. INTRODUCTION

Traumatic brain injuries (TBIs) affect ~1.7 million people, and contribute to ~30% of the annual injury related deaths in the United States alone.[1–3] Growing evidence points to a link between the severity of TBI and the increased risk of permanent physical and mental disability in people who survive a TBI.[4] While the majority of TBI cases are classified as mild, moderate-to-severe TBIs are known to contribute to the bulk of TBI associated medical costs and fatalities in the US.[3] Individuals that survive moderate-to-severe TBIs are often faced with significant long-term functional deficits due to the widespread cellular damage and neurotoxicity around the site of injury.[2,5] There are currently no effective treatments for TBI.

The pathophysiology of moderate-to-severe TBI is complex. These injuries can result from diffuse or focal damage to brain tissue that progresses in temporally distinct primary and secondary injury phases. The initial mechanical insult to brain tissue and its manifestations immediately following the injury constitutes the primary injury phase. During this period, the disruption of neurovasculature, ionic, and neurotransmitter imbalance, and impact induced cell death is observed.[5,6] The secondary injury phase that follows can persist for extended periods of time leading to adverse outcomes. This phase of the injury cascade involves the manifestation of impaired cerebral blood flow, edema, increased intracranial pressure (ICP), blood–brain barrier (BBB) breach, and excitotoxic neuronal cell death. A hallmark of the secondary injury cascade is the presentation of a heightened inflammatory response initiated by the innate immune system. This sustained inflammatory signaling by native glial cells and blood-borne immune cells ultimately culminates in significant long-term damage and necrosis of brain tissue.[6]

The current clinical standard of treatment for moderate-to-severe TBIs involves acute stabilization of the patient, and the administration of preventative treatments depending on the severity of TBI as dictated by the Glasgow Coma Scale (GCS).[7] Acute treatment of moderate-to-severe TBIs include non-invasive and invasive procedures to clear subdural and

epidural hematomas, and reduce ICP to prevent long-term neuronal damage and preserve function.[8] Pharmacological and non-pharmacological experimental therapies to combat progressive functional loss after TBI has been met with limited success so far. A majority of acute therapies (40/55) have been reported to induce adverse outcomes or show no measurable benefit of treatment.[8] There are currently no active acute interventions available to help mediate the large-scale repair and regeneration of brain tissue that is required to promote functional recovery post-TBI.

The endogenous regenerative capacity of the brain is evidenced in the ability of endogenous neural stem cells (NSCs) to proliferate and differentiate into neurons post-TBI.[9] Exogenously delivered NSCs have also been demonstrated to significantly improve functional recovery post-TBI in mice studies.[10] However, the poor survival and differentiation potential of exogenous and endogenous NSCs post-TBI has so far limited their long-term therapeutic potential. Previous evidence from inflammatory neurodegenerative disease studies suggests that undifferentiated transplanted or host NSCs trigger a “bystander effect”, wherein, undifferentiated NSCs can mediate immunomodulation and produce a host of neuro-protective factors to significantly protect neural tissue.[11] The transplantation and maintenance of undifferentiated NSCs in the lesion site could yield significant benefits over other approaches focused on inducing NSC differentiation, due to their ability to mediate neuroprotective paracrine signaling and long-term brain tissue repair post-TBI, provided strategies to maintain the undifferentiated state of NSCs can be converged upon.

The brain extracellular matrix (ECM) is uniquely different from other tissue ECMs due to the near absence of fibrous ECM proteins, and the selective abundance of “lecticans”, chondroitin sulfate proteoglycans (CSPGs) that contain lectin and hyaluronic acid (HA) binding domains.[12] Lecticans consist of a core protein to which are tethered sulfated CS-GAG side-chains consisting of a wide variety of sulfation patterns. Lecticans bind to ECM proteins such as tenascin-R and fibronectin via protein–protein interactions.[13] The associated CS-GAGs also reportedly bind collagen via mechanisms independent of the core protein.[14] In addition to facilitating ECM interactions, sulfated CS-GAGs are known to possess specific binding affinities to chemokines such as Stromal Cell-Derived Factor-1α (SDF-1α);[15] and a host of neuroprotective trophic factors such as midkine (MK), pleiotrophin (PTN), FGF, brain-derived neurotrophic factor (BDNF), epidermal growth factor (EGF), glial cell-line derived neurotrophic factor (GDNF), and ciliary neurotrophic factor (CNTF).[16,17] CS-GAGs are abundantly present in the brain NSC niches such as the sub-ventricular and the sub-granular zones (SVZ & SGZ). The selective enzymatic degradation of CS-GAGs in these brain regions, has been reported to result in the reduced proliferation and neuronal differentiation of NSCs, and enhanced differentiation into astroglia.[18,19] We have recently demonstrated that CS-GAG matrices are able to selectively bind and retain FGF2, BDNF, and the anti-inflammatory cytokine Interleukin-10 (IL-10) over a period of 15 days in vitro.[20] We have previously also demonstrated the ability to maintain the undifferentiated state of NSCs encapsulated in CS-GAG matrices in vitro.[20]

In this study, we evaluated the ability of CS-GAG matrix implants to bind and retain endogenous FGF2 and maintain the undifferentiated state of NSCs over a period of 4 weeks

post-TBI. We performed controlled cortical impact (CCI) injuries of the rat frontroparietal cortex and intraparenchymally administered allogeneic NSCs encapsulated in predominantly monosulfated CS-GAG matrices acutely (48 h) post-TBI. We evaluated the potential of matrix encapsulated NSCs in mediating neuroprotection, and endogenous repair of brain tissue 4 weeks post-TBI using histolopathological methods.

2. MATERIALS AND METHODS

2.1. Trophic Factor Enrichment in Sulfated CS and Unsulfated HA Matrices

In order to assess the enhanced ability of CS-GAG matrices to bind and retain FGF2 when compared to HA matrices, they were cast into circular holes cut out from a ~ 1 mm thick HA matrix as described below. Methacrylated CS-GAG consisting of 86% CS-4 (CS-A), 5% 6 (CS-C), 6% 4,6 (CS-E) sulfated GAGs; and HA were synthesized using methods previously reported by us.[20] One mm thick HA matrices were cast in a 35 mm cell culture dish containing a 14 mm glass bottomed microwell (Cellvis, CA). ~1 mm round disks were cut out from the HA matrices using a biopsy punch, and the holes filled in with CS-GAG matrix and photo-cross-linked as described previously.[20] The gels thus patterned were then overlaid with PBS containing 10 ng/mL FGF2, and incubated for 1 week in a standard humidified air incubator held at 37°C and 95% humidity containing 5% CO_2. After 1 week, the PBS was removed from the gels, and the gels were frozen in optimal cutting temperature (OCT) compound (Sakura Finetek, CA). Frozen gels were later sectioned using a Leica cryostat (LeicaBiosystems, IL) at 15 μm thick sections. Sections were washed thrice with PBS and immunohistochemically stained with anti FGF2 primary antibody (Abcam, MA) and appropriate secondary antibody. Fluorescein labeled *Wisteria floribunda* agglutinin (WFA; Vector Laboratories, CA) was used to mark the location of the CS-GAG matrix. Fluorescently stained matrices were imaged using epifluorescence microscopy (Leica Microsystems, IL).

2.2. Surgical Procedures and TBI Induction

All animals were approved by the Georgia Institute of Technology Institutional Animal Care and Use Committee (IACUC), and protocols were performed in accordance with the Guide for the Care and Use of Laboratory Animals published by the National Institute of Health (NIH). A total of 45 seven-week-old Sprague–Dawley (~200 g) rats were obtained from Harlan Laboratories and assigned to control and experimental groups. Nine animals served as sham controls, receiving a craniotomy but no CCI injury. The remaining 30 six animals were evenly divided into the positive control TBI group (TBI), the CS-GAG matrix implant group (GAG), the NSC injection group (NSC), and the combined CS-GAG-NSC matrix implant group (GAG-NSC). A custom-designed CCI was used to deliver the desired impact to the frontoparietal cortex of the TBI-only control and experimental animals. Prior to injury, each rat was anesthetized using 5% isoflurane gas and the head was then depilated to expose the underlying skin. The animal was then placed on a heated pad to maintain its body temperature at 37 °C, and its head was mounted into a stereotaxic frame (David Kopf Instruments, CA) with the nose placed into a nose mask that delivered the aforementioned level of surgical anesthesia. The surgical site was sanitized thrice using alternating chlorohexidine and ethanol swabs. A longitudinal incision was made such that bregma,

coronal, sagittal, and lambdoid sutures were exposed. The skin flaps and tissue was reffected on either side of the incision, and a 5 mm craniotomy was performed 0.5 mm anterior to bregma and 0.5 mm lateral from the sagittal suture using a 5 mm diameter trephine bur and an electronic drill. The bone flap was subsequently removed, noting any blood, hemorrhages, and the state of dura. A 3 mm tip attached to the pneumatic piston of the CCI was extended to its full length and positioned near the surface of the exposed dura in the top right corner of the craniotomy. The piston was retracted and lowered 2 mm, then fired at a velocity of 2.25 m/s and with a dwell time of 250 ms, resulting in a 3 mm diameter injury with a depth of 2 mm (Figure S1). A saline soaked piece of gelfoam was applied to the injury site, and sterile cotton swabs were used to remove any excess blood. The gel foam was subsequently removed, and the injury site was covered completely with a layer of 2% SeaKem agarose (Lonza, MD). The skin flaps were subsequently sutured together to close the wound, and triple antibiotic cream was layered on top of the sutured skin. Buprenorphine (1 mg/kg) was injected subcutaneously before animals were removed from anesthesia and placed in a new, clean cage under a heating lamp to recover. The animals were returned to their home cages after recovery.

2.3. NSC Culture

Primary rat NSCs isolated at embryonic day 14 (MTI-GlobalStem, MD) were subcultured in ES-DMEM-F12 (MTI-GlobalStem, MD) containing N2 supplement and 10 ng/mL FGF2. The cultures were maintained in a standard humidified air incubator held at 37 °C and 95% humidity containing 5% CO_2, and culture media was replaced every 2 days. After approximately 3–4 days when plates reached about 90% confluence, cells were rinsed thrice using 20 mM HEPES Buffered Salt Solution (HBSS) lacking calcium or magnesium (Corning, NY) and scraped from the culture dish using a cell scraper to detach the cells. The detached cells were centrifuged at 270*g* for 5 min and the pellet was resuspended in ES-DMEM/F12. The cells were counted using an automated cell counter (Bio-Rad, CA) and prepared for encapsulation and delivery as described below.

2.4. Intraparenchymal Injection of Matrices and Matrix Encapsulated NSCs

Two days post-TBI, injured animals were randomly assigned to either the positive control TBI group ($n = 9$) or one of the three experimental groups GAG, NSC, or GAG-NSC ($n = 9$ per group). CS-GAG matrices with or without PKH26GL (SigmaAldrich, MO) labeled NSCs were photo-cross-linked on the day of injection using previously described methods.[20] In the case of animals receiving NSCs only, ~300 000 PKH26GL labeled rat NSCs were resuspended in basal media (20 μL volume), and delivered using methods below. For animals receiving CS-GAG matrix-only controls, 20 μL of 3% w/v CS-GAG matrix in neurobasal media containing 0.05% photoinitiator (Irgacure-2959, Sigma-Aldrich, MO) was back-filled into a 50 μL Luer Lock (TLL) Hamilton syringe fitted with a BD Visitec Nucleus Hydrodissector needle (BD Medical, NJ). The solution was subsequently cross-linked in the syringe by exposing it to 365 nm long wavelength UV light (160 W BlakRay UVP, CA) for 30 s and prepared for intraparenchymal delivery as described below. For animals receiving NSC laden CS-GAG matrices, 300 000 NSCs were resuspended in 20 μL 3% (w/v) methacrylated CS-GAG in neurobasal media containing 0.05% photoinitiator

(Irgacure-2959,) and back-loaded into a 50 μL Hamilton syringe as described above and prepared for delivery as described below.

The animals were prepared for intraparenchymal injections by placing them under surgical anesthesia as described above. The incision area was sanitized using ethanol and chlorhexidine as described above, and the sutures were removed to reffect the skin flaps. The 2% agarose matrix was carefully removed from the injury site using sterile saline soaked cotton swabs, without disturbing the underlying brain tissue. For each treatment containing NSCs only, CS-GAG only, or GAG-NSCs, the syringe was fitted onto a syringe pump and assembled on an electrode manipulator (David Kopf, CA) at a 32° angle. The needle tip was then implanted in the injury epicenter to a depth of 2 mm. A 20 μL volume of the matrix was delivered at a rate of 2 μL per minute, over a period of 10 min using the syringe pump. After 10 min, the needle was held in place for 5 min and then gradually retracted. The surface of the cortex was kept moist with a piece of gel foam soaked in saline during the course of this procedure. The gelfoam was subsequently removed, and the craniotomy was overlaid with 2% agarose as described above and covered with UV curing dental cement. The skin flaps were sutured and the animal was allowed to recover as described above.

2.5. Neural Tissue Preparation and Immunohistochemistry

Four weeks postinjury, animals were heavily sedated using ketamine (65 mg/kg) and transcardially perfused with 250 mL PBS (pH 7.4) followed by 250 mL of 4% paraformaldehyde in PBS, and finally with 100 mL 20% sucrose in PBS. The brains were then extracted and cut at the epicenter of the lesion using a rat brain matrix (Ted Pella Inc., CA) to result in two halves. Each half section was frozen fresh first in liquid nitrogen and then stored at −80 °C. The extracted brains were sectioned at 15 μm thickness using a cryostat (LeicaBiosystems, IL), collecting 10 slides per animal (5 slides from the rostral side of the injury and 5 from the caudal side) (Figure S2). Immunohistochemical staining of cryostat sectioned brain slices was performed using primary and secondary antibody pairs as described in Table 1, and using methods previously described.[21,22]

Brain sections collected on glass slides, were rinsed in PBS and subsequently incubated in PBS containing 4% paraformaldehyde and 0.4 M sucrose for 30 min. The slides were then assigned to primary antibody groups and incubated for 1 h in blocking buffer (PBS containing 4% goat serum and 0.5% Triton-X100), followed by overnight incubation in blocking buffer containing appropriate antibodies (Table 1). The following day, the slides were washed several times in PBS at room temperature and exposed to blocking buffer for 1 h at room temperature. Slides were then incubated with blocking buffer consisting of 1:220 dilutions of appropriate secondary antibodies for 1 h. Following incubation, slides were washed several times in PBS. 500 μL NucBlue (Life Technologies, NY) in PBS was added to each slide for 5 min at room temperature. Slides were rinsed thrice with PBS and coverslipped using Fluormount-G (Southern Biotech, AL). Sections were allowed to cure overnight, and stored at −20 °C until imaged.

Nissl bodies in brain sections were stained using cresyl violet stain (SigmaAldrich, MO). Sections were placed in PBS containing 4% paraformaldehyde containing 0.4 M sucrose for 30 min. The fixed sections were rinsed thrice in PBS, and air-dried following which they

were immersed in a 1:1 solution of alcohol and chloroform. The next day, the sections were sequentially rehydrated through 100%, and 95% EtOH, and finally into DiH_2O. The sections were subsequently labeled with 0.1% cresyl violet solution for 5–10 min to stain for Nissl bodies in neurons. The stained sections were cleared by passing them sequentially through DiH_2O, 70, 95, and 100% EtOH. The dehydrated sections were finally cleared in xylene and coverslipped with permount (Fisher Scientific, NC), and allowed to cure overnight at room temperature.

2.6. Quantification of Immunofluorescence

Cresyl violet stained slides marking nissl bodies were imaged at the coronal epicenter of the injury using a light microscope (Nikon bright field and Q-Imaging software). The region of interest (ROI) represented 10.494 mm^2, and four images were taken per animal ($n = 9$; 36 total images). ImageJ was used to determine and analyze the number of marked nissl bodies, thresholding to signal peak (~200) and using the subtraction tool to eliminate any noise. For immunofluorescent slides, five sections spanning the injury site were imaged using epifluorescence microscopy (LeicaBiosystems, IL), and fluorescence staining intensity was quantified using Volocity (PerkinElmer, MA). The Manders overlap coefficient was used to measure the degree of overlap and colocalization between dual-colored fluorescent images, as it is a better indicator of co-occurrence when compared to other methods.[29] It is represented by the equation

$$\frac{\sum_i (R_i X G_i)}{\sqrt{\sum_i R_i^2 X \sum_i G_i^2}}$$

Where R_i and G_i are the fluorescence intensity values of the red and green channels in a pixel "i", respectively.

2.7. Statistical Analysis

All statistical inferences for CS-GAG enrichment and immunohistochemical assays were made using SigmaPlot (SyStat Software, Inc., CA). Student's *t*-test, one way analysis of variance (ANOVA), and a one-way repeated measures ANOVA on ranks with multiple pairwise comparisons and relevant posthoc tests were applied as deemed appropriate. For all tests, $p < 0.05$ was considered significant.

3. RESULTS

3.1. FGF2 Retention in CS and HA Matrices

Because HA is a major unsulfated GAG present in the brain tissue ECM in addition to sulfated CS-GAGs, we investigated the extent of FGF2 binding to HA and CS-GAG matrices when presented in solution simultaneously to both matrices. We patterned HA and CS-GAG matrices as described in the methods above, and performed immunohistochemical analysis using fluorescein conjugated WFA lectin to label the CS-GAG matrix, and antibody labeling of FGF2 bound to CS-GAG and HA matrices as described above. Results from

these assays qualitatively demonstrate the enhanced WFA^+ staining of the CS-GAG matrix when compared to the HA matrix (Figure 1B). These results also demonstrate that FGF2 bound preferentially to the CS-GAG matrix when compared to HA matrix (Figure 1C, D). The colocalization of FGF2 with CS-GAGs is also evidenced in the adult rat SVZ (Figure S3). When compared to the cortex, we observed a significantly ($p < 0.001$) higher percentage colocalization of FGF2 with WFA^+ brain tissue in the SVZ (Figure S3A). No significant differences were observed between the Ki67/WFA^+ and FGF2/WFA^+ tissue in the rat SVZ (Figure S3B). A high correlation of Ki67/WFA^+ tissue with FGF2/WFA^+ tissue was observed in the rat SVZ (Figure S3C).

3.2. CS-GAG Matrix Induced Neuroprotection of Brain Tissue 4 Weeks Post-TBI

To evaluate the extent of neural tissue loss 4 weeks post-TBI, we performed cresyl violet staining of coronal brain tissue sections. A qualitative comparison of neuronal presence in brain tissue indicated that TBI and NSC-only treated control animals experienced extensive neuronal loss as evidenced by the lack of neural tissue and Nissl staining in the region surrounding the impacted site (Figure 2A, B). In comparison, the GAG only and GAG-NSC treated animals demonstrated a healthy presence of neuronal tissue, as indicated by the significantly higher presence of cresyl violet labeled Nissl bodies in the region surrounding the CCI impact (Figure 2C, D), when compared to control TBI and NSC only treated animals. To quantify the extent of neuronal loss across these treatments, we counted Nissl bodies using methods presented above. The extent of neuronal loss in sham, NSC, GAG, and GAG-NSC treated animals were compared to the control TBI only treated animals. Results from these analyses demonstrate that the sham, GAG, and GAG-NSC groups have significantly ($p < 0.05$) greater presence of neurons as indicated by positive Nissl staining when compared to TBI only treated animals (Figure 2E). Pairwise multiple comparisons between all groups also indicate that both the GAG and GAG-NSC treated animals demonstrate significantly ($p < 0.05$) greater neuronal presence as indicated by positive Nissl staining when compared to the control TBI only, and NSC only treated animals (Figure 2E). The NSC treated animals showed significantly ($p < 0.05$) lesser Nissl staining when compared to sham control. However, no significant differences in Nissl staining were observed between the sham, and GAG-NSC groups; and between the GAG and GAG-NSC groups.

3.3. Survival and proliferation of NSCs transplanted in CS-GAG Matrices 4 weeks post -TBI

The survival and proliferation of PKH26GL-labeled allogenic rat NSCs delivered either alone or encapsulated in CS-GAG matrices was evaluated using immunohistochemical techniques as described above. Our results demonstrate the significantly higher retention of NSCs in the lesion area when encapsulated and delivered in CS-GAG matrices when compared to NSCs delivered in basal media, as demonstrated by the significantly ($p < 0.01$) greater colabeling of the cell-membrane dye PKH26GL with the NSC marker Sox1 4 weeks post-TBI (Figure 3A–C). NSCs delivered in CS-GAG matrices also demonstrated a significantly ($p < 0.01$) greater number of cells colabeled for PKH26GL and the cell proliferation marker Ki67 (Figure 3A, B, D).

3.4. Local Retention of FGF2 and Maintenance of the Undifferentiated State of NSCs in CS-GAG Matrices 4 Weeks Post-TBI

Quantitative immunohistochemical analysis of brain tissue 4 weeks post-TBI indicated that animals implanted with CS-GAG matrices alone, or with CS-GAG matrices carrying NSCs demonstrated significantly ($p < 0.05$) greater local FGF2 retention when compared to sham and TBI controls, and NSC only treated animals (Figure 4A, B). A quantitative analysis of cell differentiation of transplanted cells indicated that a significantly high number of PKH26GL labeled cells expressed the NSC marker Sox1 when compared to the neuronal differentiation marker NeuN, and the oligodendrocyte marker Olig2 (Figure 5A, B). $NeuN^+$ cells in GAG-NSC treated animals also demonstrated the complete absence of NF200 staining for neurofilaments typically present in the neuronal cytoskeleton of mature neurons (Figure. S4). High-magnification images of transplanted NSCs indicated a high degree of colocalization of the cell membrane marker PKH26GL with the NSC markers Sox1 and nestin (Figure 5C).

3.5. Inflammatory Response and Astroglial Scarring Mediated by Implanted Matrices

To assess the extent of inflammatory response and astroglial scarring mediated by CS-GAG matrix implants 4 weeks post-TBI, we performed immunohistochemical staining of coronal sections using antibodies against GFAP for reactive astrocytes, and CD68 for activated macrophages. Due to the large extent of necrotic tissue loss observed in the brain tissue explanted from TBI-only control animals, the localization of $CD68^+$ cells was confined to the lesion boundaries as depicted in Figure 6A. In comparison, CD68+ cells were distributed throughout the matrix in the GAG-NSC treated group (Figure 6A). A quantification of $CD68^+$ cells in the brain tissue of CS-GAG matrix implanted animals showed a significant increase in cellular presence in the NSC and GAG-NSC treated animals when compared to sham, TBI, and GAG matrix treated animals (Figure 6B). In contrast, the presence of reactive astrocytes was observed to be the highest in coronal sections obtained from the TBI-only control animals, as evaluated by the fluorescence intensity analysis when compared to all other treatments (Figure 6C). There were no significant differences in GFAP fluorescence intensity observed between the treatment groups and the sham control animals (Figure 6C). Interestingly, GFAP staining in the matrix treated animals was confined to the lesion boundary (Figure 6A), and GFAP+ reactive astrocytes did not appear to infiltrate the matrix.

DISCUSSION

Despite tremendous efforts, there are currently no therapeutics that can actively promote the repair and regeneration of brain tissue after moderate-to-severe TBIs. In order to help bridge this gap, we sought to better understand the essential components of the brain ECM, with the intent of developing a biomaterial construct that could help integrate with brain tissue, and simultaneously provide trophic support to promote repair and regeneration after traumatic insults to the brain. We recently developed a CS-GAG matrix based delivery construct that is entirely composed of sulfated CS-GAGs native to brain ECM, and which possess important functional sulfate groups that can regulate NSC behavior.[20] In this study, we administered these constructs either alone or laden with NSCs intraparenchymally into the rat cortex acutely after a moderate-to-severe TBI, and investigated their ability to facilitate neural

tissue repair 4 weeks post-TBI. We demonstrate that CS-GAG matrices when delivered alone or in combination with NSCs, significantly enhance neuroprotection and brain tissue repair subacutely post-TBI.

The neuroprotective effects of transplanted NSCs after TBI have been well documented.[30] However, there is much debate about whether it is the bystander signaling mediated paracrine effects mediated by NSCs, or the targeted differentiation of transplanted NSCs that ultimately contribute to enhanced recovery after TBI. Despite several years of research focused on the development of stem cell therapies, their clinical application to provide cell replacement after injury or disease remains to be realized. Evidence from studies on CNS injury and inflammatory models of neurodegenerative diseases seem to suggest that it is the paracrine effects rather than direct cell replacement by NSCs that significantly contribute to the repair and recovery of the injured or diseased CNS.[11] However, a number of factors including the timing and mode of cell transplantation need to be considered to ensure maximum survival and efficacy of transplanted NSCs. The precise timing of NSC transplantation post-TBI is critical to ensuring the maximum survival and differentiation potential of transplanted cells. A time window of 2–7 days post-TBI has been determined to be the optimal time for NSC transplantation.[30] NSCs encapsulated in ECM scaffolds composed of laminin and fibronectin were demonstrated to undergo better survival and distribution when compared to NSCs delivered in media alone post-TBI, indicating that matrix encapsulation both protects and controls the differentiation potential of transplanted NSCs.[31] In previous in vitro studies, we have demonstrated the ability of CS-GAG matrices to enhance the paracrine effects of NSCs and promote the self-renewal and proliferation of matrix encapsulated NSCs.[20] Our results from this study corroborate previous findings, and further demonstrate that in addition to facilitating the survival and proliferation of transplanted NSCs, animals treated with CS-GAG matrices either alone or with encapsulated NSCs significantly enhanced neuroprotection of brain tissue 4 weeks post-TBI.

FGF2 is known to promote mitogenesis of NSCs, and is essential for their subsequent neuronal differentiation.[32] FGF2 is also upregulated locally in areas of brain tissue injury, where it is believed to promote both the proliferation and differentiation of NSCs, and protects differentiated neurons from degradation after TBI.[23] FGF2 gradients present within germinal niches of the adult and developing central nervous system (CNS) are responsible for restricting self-renewing NSCs to these areas of the brain.[24] When compared to heparin sulfate proteoglycans (HSPGs) the role of CSPGs and their associated CS-GAGs in binding growth factors, and in inducing cellular haptotaxis has received little attention. However, the relative overabundance of CSPGs and their associated CS-GAGs in brain ECM when compared to HS-GAGs, prompts further investigation into their role in promoting local growth factor retention and in regulating cell proliferation and differentiation. Unsulfated GAGs such as HA and monosulfated CS-A and C are found to be equally distributed in the white matter.[33] However, the specialized role played by CS in promoting the sulfation specific binding of trophic factors and trophic factor signaling in the brain ECM when compared to relevant unsulfated GAGs such as HA has been the subject of little scrutiny. Previous reports indicate that the CSPG phosphacan binds FGF2 and potentiates its mitogenic activity in levels comparable to heparin.[34] Other reports also indicate that the sulfated CS-GAGs alone can bind and immobilize FGF2, and that the extent of binding is

sulfation dependent, with the disulfated CS-E demonstrating higher FGF2 affinity when compared to monosulfated CS-GAGs.[16,17,20] Sirko et. al, demonstrated that the selective removal of the sulfated CS-GAG chains via chondroitinase ABC treatment reduced NSC self-renewal and neuronal differentiation, and instead promoted astroglial differentiation.[18,19] Given these previous findings, we attempted to create an ectopic niche composed entirely of sulfated CS-GAGs to help promote the survival, and prolong the paracrine effects of both transplanted and endogenous NSCs post-TBI. Our results corroborate these findings, and demonstrate that sulfated CS-GAGs are abundantly present in the adult rat SVZ when compared to the cortex. Our results support our previous findings,[20] and demonstrate that the FGF2 binds selectively to CS-GAG matrices and not to control unsulfated HA matrices when presented simultaneously to both matrices. These results also represent the natural affinity and localization of FGF2 in the white matter where CS-GAGs and HA are equally distributed. We also demonstrate that implanted sulfated CS-GAG matrices are capable of mediating the enhanced binding and retention of FGF2 in the lesion site 4 weeks post-TBI, which may have contributed to the significantly enhanced presence of self-renewing (Sox1+ and nestin+) NSCs in this region when compared to differentiated neural cells in GAG-NSC treated animals 4 weeks post-TBI. In NSCs that differentiated into neurons (NeuN+), we observed the complete lack of NF200 staining, indicating that these cells had not yet differentiated into mature neurons. These results suggest that endogenous or transplanted $Sox1^+$ cells present within the CS-GAG matrix implants could potentially be producing FGF2 and contributing to localized FGF2 retention mediated maintenance of undifferentiated NSCs in CS-GAG matrices.

Traumatic insults to the CNS result in the accumulation of $GFAP^+$ hypertrophic reactive astrocytes around the lesion site, which is commonly referred to as astroglial scarring.[35] The presence of astroglial scar around the lesion site acts as molecular barrier due to the local overexpression of nerve inhibitory CSPGs by the reactive astrocytes. However, recent evidence suggests that several neuronal growth promoting CSPGs are also associated with astroglial scar and that the attenuation or complete ablation of astroglial scar surrounding spinal cord lesions proved detrimental to axonal regeneration.[36] In order to decipher whether or not astroglial scar has similar implications for repair and regeneration of brain lesions, the compositional and functional complexity of scar associated CSPGs and CS-GAGs surrounding brain lesions needs to be fully investigated. Our previous findings suggest that sulfated CS-GAGs linked to CSPGs could play an important role in regulating neuronal growth promotion and inhibition in brain lesions.[37] We had previously demonstrated that the disulfated CS-E associated with astroglial scar is a potent inhibitor of neuronal regeneration,[37,38] and that monosulfated CS-GAGs such as CS-A do not play a role in this mechanism.[37] Monosulfated CS-GAGs such as CS-A are abundantly present in the uninjured brain tissue, and are essential components required for the maintenance and self-renewal of NSCs in the germinal niches of the brain.[33] Our results support these findings and demonstrate that animals treated with CS-GAG matrices composed predominantly of CS-A induced a significantly attenuated astroglial scarring of brain tissue surrounding the matrix implant when compared to brain tissue obtained from TBI-only control animals, which showed a more compact astroglial scar surrounding the lesion site, and heightened presence of GFAP+ astrocytes. The delivery of trophic factor enriching CS-GAG matrices directly into the

epicenter of TBI lesions may therefore help create the necessary environmental conditions required to promote the repair and regeneration of lesioned brain tissue post-TBI via mechanisms separate from those required to promote long-distance axonal regeneration after spinal cord lesions.

In addition to reactive astrocytes, the breach of the BBB induces the infiltration of a host of blood-borne myeloid cells including macrophages. The acute infiltration of CD-68+ activated macrophages has been reported to contribute significantly to the pathophysiology of TBI, where they are responsible for activating temporally distinct pro- and anti-inflammatory immune responses.[39] The acute presence of pro-inflammatory phagocytic M1-like macrophages was demonstrated to increase in presence during the acute phase comprising the first 10–14 days post-TBI.[39] Cytotoxic responses triggered by microglia and activated macrophages have been linked to the observed progressive tissue necrosis observed following brain trauma.[40] Our results demonstrated a significantly higher presence of CD68+ macrophages in NSC treated animals (NSC, and GAG-NSC groups) indicating that allogeneic NSC transplants do induce an immune response in vivo. Interestingly, animals implanted with the CS-GAG matrix alone did not demonstrate this heightened activated macrophage response, suggesting that it might be a promising candidate for brain tissue repair applications. In contrast to the significant loss of brain tissue and tissue cavitation observed at the lesion epicenter in brain tissue obtained from TBI control and NSC treated animals, the significantly enhanced preservation of brain tissue and Nissl bodies in animals treated with CS-GAG matrices seems to suggest a largely neuroprotective role for these scaffolds. A more in-depth molecular analysis of the inflammatory milieu surrounding these scaffolds, and the effects of acute, subacute, and chronic neuroprotection on animal behavior and functional recovery are currently ongoing.

CONCLUSIONS

In summary, our results demonstrate that (a) sulfated CS-GAG matrices selectively bind and sequester FGF2 when compared to unsulfated HA matrices, and exhibit similar bioactive properties to native ECM in the SVZ; (b) when delivered intraparenchymally into the cortex of TBI impacted rats, CS-GAG matrices promote neuroprotection and significantly enhance the survival and proliferation of transplanted NSCs 4 weeks post-TBI; (c) CS-GAG matrix implants promote FGF2 retention and promote the maintenance of the undifferentiated state of matrix encapsulated NSCs; and d)animals implanted with CS-GAG matrices induced a significantly attenuated inflammatory response, and reduced astroglial scarring response when compared to TBI control and NSC only treated animals. These results provide evidence to support the role of sulfated CS-GAGs in facilitating trophic factor signaling to promote NSC efficacy, and provide justification for their use as neuroprotective matrices that can be administered acutely to promote the repair and regeneration of brain tissue after a moderate-to-severe TBI.

Supplementary Material

Refer to Web version on PubMed Central for supplementary material.

Acknowledgments

This research was supported by startup funds awarded to L.K. by the University of Georgia CAES and OVPR, and in part by seed grant funding from the Georgia Institute of Technology/Emory University Regenerative Engineering and Medicine Center and The University of Georgia awarded to R.V.B. and L.K. This work is also supported in part by the National Center for Advancing Translational Sciences of the National Institutes of Health under award number UL1TR00454. The National Institutes of Health (NIH/NCRR)-funded grant entitled 'Integrated Technology Resource for Biomedical Glycomics' (Grant 1 P41 RR018502-01) to the Complex Carbohydrate Research Center, The University of Georgia.

References

1. CDC. Grand Rounds: Reducing Severe Traumatic Brain Injury in the United States. Morbidity and Mortality Weekly Report. 2013; 62(27):549–552. [PubMed: 23842444]
2. Faul, M., Xu, L., Wald, M., Coronado, V. Traumatic Brain Injury in the United States: Emergency Department Visits, Hospitalizations and Deaths 2002–2006. National Center for Injury Prevention and Control, Centers for Disease Control and Prevention; Atlanta, GA: 2010.
3. Saatman KE, Duhaime AC, Bullock R, Maas AI, Valadka A, Manley GT. Classification of traumatic brain injury for targeted therapies. J Neurotrauma. 2008; 25(7):719–738. [PubMed: 18627252]
4. Maas AI, Stocchetti N, Bullock R. Moderate and severe traumatic brain injury in adults. Lancet Neurol. 2008; 7(8):728–41. [PubMed: 18635021]
5. McIntosh TK, Saatman KE, Raghupathi R, Graham DI, Smith DH, Lee VM, Trojanowski JQ. The Dorothy Russell Memorial Lecture. The molecular and cellular sequelae of experimental traumatic brain injury: pathogenetic mechanisms. Neuropathol Appl Neurobiol. 1998; 24(4):251–67. [PubMed: 9775390]
6. Helmy A, De Simoni MG, Guilfoyle MR, Carpenter KL, Hutchinson PJ. Cytokines and innate inflammation in the pathogenesis of human traumatic brain injury. Prog Neurobiol. 2011; 95(3): 352–72. [PubMed: 21939729]
7. Bruns J Jr, Hauser WA. The epidemiology of traumatic brain injury: a review. Epilepsia. 2003; 44(Suppl 10):2–10.
8. Lu J, Gary KW, Neimeier JP, Ward J, Lapane KL. Randomized controlled trials in adult traumatic brain injury. Brain Injury. 2012; 26(13–14):1523–1548. [PubMed: 23163248]
9. Rice AC, Khaldi A, Harvey HB, Salman NJ, White F, Fillmore H, Bullock MR. Proliferation and neuronal differentiation of mitotically active cells following traumatic brain injury. Exp Neurol. 2003; 183(2):406–417. [PubMed: 14552881]
10. Riess P, Zhang C, Saatman KE, Laurer HL, Longhi LG, Raghupathi R, Lenzlinger PM, Lifshitz J, Boockvar J, Neugebauer E, Snyder EY, McIntosh TK. Transplanted neural stem cells survive, differentiate, and improve neurological motor function after experimental traumatic brain injury. Neurosurgery. 2002; 51(4):1043–1054. discussion 1052–4. [PubMed: 12234415]
11. Martino G, Pluchino S. The therapeutic potential of neural stem cells. Nat Rev Neurosci. 2006; 7(5):395–406. [PubMed: 16760919]
12. Ruoslahti E. Brain extracellular matrix. Glycobiology. 1996; 6(5):489–92. [PubMed: 8877368]
13. Aspberg A, Miura R, Bourdoulous S, Shimonaka M, Heinegard D, Schachner M, Ruoslahti E, Yamaguchi Y. The C-type lectin domains of lecticans, a family of aggregating chondroitin sulfate proteoglycans, bind tenascin-R by protein-protein interactions independent of carbohydrate moiety. Proc Natl Acad Sci U S A. 1997; 94(19):10116–21. [PubMed: 9294172]
14. Toole BP. Binding and precipitation of soluble collagens by chick embryo cartilage proteoglycan. J Biol Chem. 1976; 251(3):895–897. [PubMed: 129475]
15. Logun MT, Bisel NS, Tanasse EA, Zhao WJ, Gunasekera B, Mao LD, Karumbaiah L. Glioma cell invasion is significantly enhanced in composite hydrogel matrices composed of chondroitin 4-and 4,6-sulfated glycosaminoglycans. J Mater Chem B. 2016; 4(36):6052–6064. [PubMed: 28217304]
16. Deepa SS, Umehara Y, Higashiyama S, Itoh N, Sugahara K. Specific molecular interactions of oversulfated chondroitin sulfate E with various heparin-binding growth factors. Implications as a physiological binding partner in the brain and other tissues. J Biol Chem. 2002; 277(46):43707–16. [PubMed: 12221095]

17. Nandini CD, Mikami T, Ohta M, Itoh N, Akiyama-Nambu F, Sugahara K. Structural and functional characterization of oversulfated chondroitin sulfate/dermatan sulfate hybrid chains from the notochord of hagfish. Neuritogenic and binding activities for growth factors and neurotrophic factors. J Biol Chem. 2004; 279(49):50799–809. [PubMed: 15385557]
18. Sirko S, von Holst A, Weber A, Wizenmann A, Theocharidis U, Gotz M, Faissner A. Chondroitin sulfates are required for fibroblast growth factor-2-dependent proliferation and maintenance in neural stem cells and for epidermal growth factor-dependent migration of their progeny. Stem Cells. 2010; 28(4):775–87. [PubMed: 20087964]
19. Sirko S, von Holst A, Wizenmann A, Gotz M, Faissner A. Chondroitin sulfate glycosaminoglycans control proliferation, radial glia cell differentiation and neurogenesis in neural stem/progenitor cells. Development. 2007; 134(15):2727–38. [PubMed: 17596283]
20. Karumbaiah L, Enam SF, Brown AC, Saxena T, Betancur MI, Barker TH, Bellamkonda RV. Chondroitin Sulfate Glycosaminoglycan Hydrogels Create Endogenous Niches for Neural Stem Cells. Bioconjugate Chem. 2015; 26(12):2336–2349.
21. Karumbaiah L, Saxena T, Carlson D, Patil K, Patkar R, Gaupp EA, Betancur M, Stanley GB, Carin L, Bellamkonda RV. Relationship between intracortical electrode design and chronic recording function. Biomaterials. 2013; 34(33):8061–74. [PubMed: 23891081]
22. Saxena T, Karumbaiah L, Gaupp EA, Patkar R, Patil K, Betancur M, Stanley GB, Bellamkonda RV. The impact of chronic blood-brain barrier breach on intracortical electrode function. Biomaterials. 2013; 34(20):4703–13. [PubMed: 23562053]
23. Yoshimura S, Teramoto T, Whalen MJ, Irizarry MC, Takagi Y, Qiu J, Harada J, Waeber C, Breakefield XO, Moskowitz MA. FGF-2 regulates neurogenesis and degeneration in the dentate gyrus after traumatic brain injury in mice. J Clin Invest. 2003; 112(8):1202–10. [PubMed: 14561705]
24. Palmer TD, Ray J, Gage FH. FGF-2-responsive neuronal progenitors reside in proliferative and quiescent regions of the adult rodent brain. Mol Cell Neurosci. 1995; 6(5):474–486. [PubMed: 8581317]
25. Kan L, Jalali A, Zhao LR, Zhou X, McGuire T, Kazanis I, Episkopou V, Bassuk AG, Kessler JA. Dual function of Sox1 in telencephalic progenitor cells. Dev Biol. 2007; 310(1):85–98. [PubMed: 17719572]
26. He Z, Cui L, Paule MG, Ferguson SA. Estrogen Selectively Mobilizes Neural Stem Cells in the Third Ventricle Stem Cell Niche of Postnatal Day 21 Rats. Mol Neurobiol. 2015; 52(2):927–33. [PubMed: 26041664]
27. Karimi-Abdolrezaee S, Eftekharpour E, Wang J, Schut D, Fehlings MG. Synergistic effects of transplanted adult neural stem/progenitor cells, chondroitinase, and growth factors promote functional repair and plasticity of the chronically injured spinal cord. J Neurosci. 2010; 30(5): 1657–76. [PubMed: 20130176]
28. Koppe G, Bruckner G, Hartig W, Delpech B, Bigl V. Characterization of proteoglycan-containing perineuronal nets by enzymatic treatments of rat brain sections. Histochem J. 1997; 29(1):11–20. [PubMed: 9088941]
29. Manders EMM, Verbeek FJ, Aten JA. Measurement of Colocalization of Objects in Dual-Color Confocal Images. J Microsc. 1993; 169:375–382.
30. Shear DA, Tate CC, Tate MC, Archer DR, LaPlaca MC, Stein DG, Dunbar GL. Stem cell survival and functional outcome after traumatic brain injury is dependent on transplant timing and location. Restor Neurol Neurosci. 2011; 29(4):215–225. [PubMed: 21697596]
31. Tate CC, Shear DA, Tate MC, Archer DR, Stein DG, LaPlaca MC. Laminin and fibronectin scaffolds enhance neural stem cell transplantation into the injured brain. J Tissue Eng Regener Med. 2009; 3(3):208–17.
32. Yoshimura S, Takagi Y, Harada J, Teramoto T, Thomas SS, Waeber C, Bakowska JC, Breakefield XO, Moskowitz MA. FGF-2 regulation of neurogenesis in adult hippocampus after brain injury. Proc Natl Acad Sci U S A. 2001; 98(10):5874–9. [PubMed: 11320217]
33. Akita K, von Holst A, Furukawa Y, Mikami T, Sugahara K, Faissner A. Expression of multiple chondroitin/dermatan sulfotransferases in the neurogenic regions of the embryonic and adult

central nervous system implies that complex chondroitin sulfates have a role in neural stem cell maintenance. Stem Cells. 2008; 26(3):798–809. [PubMed: 18079434]

34. Milev P, Monnerie H, Popp S, Margolis RK, Margolis RU. The core protein of the chondroitin sulfate proteoglycan phosphacan is a high-affinity ligand of fibroblast growth factor-2 and potentiates its mitogenic activity. J Biol Chem. 1998; 273(34):21439–21442. [PubMed: 9705269]
35. Silver J, Miller JH. Regeneration beyond the glial scar. Nat Rev Neurosci. 2004; 5(2):146–56. [PubMed: 14735117]
36. Anderson MA, Burda JE, Ren Y, Ao Y, O'Shea TM, Kawaguchi R, Coppola G, Khakh BS, Deming TJ, Sofroniew MV. Astrocyte scar formation aids central nervous system axon regeneration. Nature. 2016; 532(7598):195–200. [PubMed: 27027288]
37. Karumbaiah L, Anand S, Thazhath R, Zhong YH, Mckeon RJ, Bellamkonda RV. Targeted Downregulation of N-Acetylgalactosamine 4-sulfate 6-O-sulfotransferase Significantly Mitigates Chondroitin Sulfate Proteoglycan-Mediated Inhibition. Glia. 2011; 59(6):981–996. [PubMed: 21456043]
38. Gilbert RJ, McKeon RJ, Darr A, Calabro A, Hascall VC, Bellamkonda RV. CS-4,6 is differentially upregulated in glial scar and is a potent inhibitor of neurite extension. Mol Cell Neurosci. 2005; 29(4):545–558. [PubMed: 15936953]
39. Wang G, Zhang J, Hu X, Zhang L, Mao L, Jiang X, Liou AK, Leak RK, Gao Y, Chen J. Microglia/macrophage polarization dynamics in white matter after traumatic brain injury. J Cereb Blood Flow Metab. 2013; 33(12):1864–74. [PubMed: 23942366]
40. Lenzlinger PM, Morganti-Kossmann MC, Laurer HL, McIntosh TK. The duality of the inflammatory response to traumatic brain injury. Mol Neurobiol. 2001; 24(1–3):169–181. [PubMed: 11831551]

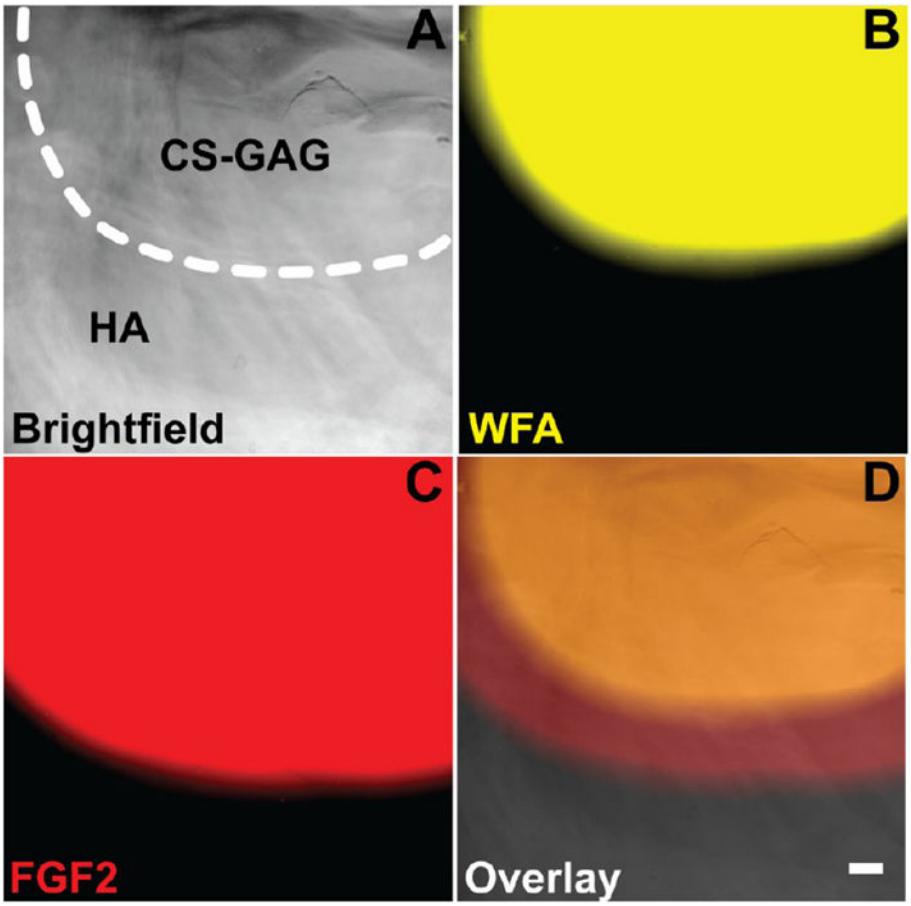

Figure 1.

Selective binding and retention of FGF2 to ~1 mm diameter CS-GAG matrix surrounded by HA matrix. (A) Bright-field image of the interface (indicated by white dotted line) of the CS-GAG and HA matrices. (B) *Wisteria f loribunda* (WFA) agglutinin labeling (pseudocolored yellow) of CS-GAG matrix. (C) Area of FGF2 binding and retention (pseudocolored red); (D) Overlay of WFA and FGF2 labeling demonstrating the preferential FGF2 binding and retention in the CS-GAG matrix when compared to surrounding HA matrix. Scale = 100 μm.

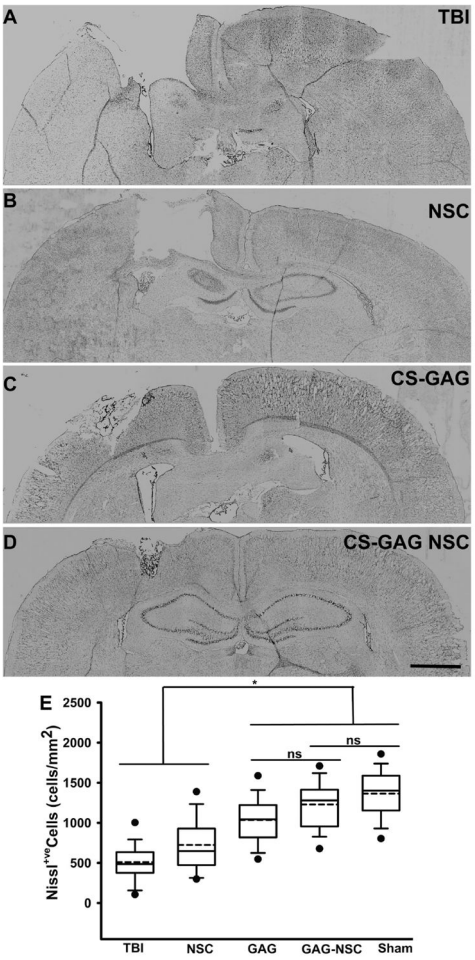

Figure 2.

Nissl staining to demonstrate the extent of neuronal presence in coronal brain sections obtained 4 weeks post-TBI from (A) TBI only control; (B) NSC only; (C) CS-GAG only; and (D) CS-GAG-NSC treatments. (E) Brain sections from CS-GAG only and CS-GAG-NSC treatments demonstrate significantly enhanced neuronal presence when compared to TBI control and NSC only treatments. Statistical significance is represented by '*', which indicates $p < 0.05$. The lack of statistical significance between groups is denoted by 'n.s'. Scale = 1 mm.

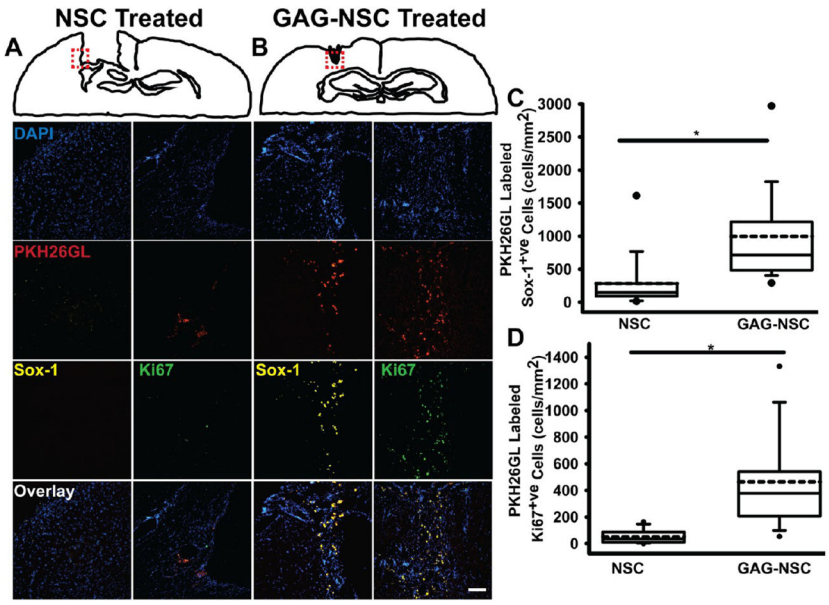

Figure 3.

Transplanted NSCs survive and proliferate 4 weeks post-TBI. Representative images of the region corresponding to the red dotted box surrounding the lesion area in coronal brain sections obtained from (A) NSC only, and (B) CS-GAG-NSC treated animals. Cellular nuclei are represented by DAPI (blue); transplanted NSCs are represented by PKH26GL labeled cells (red); undifferentiated NSC are represented by Sox1 labeling (yellow); proliferating NSCs are represented by Ki67 labeling (green). Merged overlays are presented in the bottom most panel. Significantly greater PKH26GL+ Sox1+ (C), and Ki67+ (D) NSCs were visualized in CS-GAG-NSC treated animals when compared to NSC only treated animals. Statistical significance is represented by '*', which indicates $p < 0.05$. Scale = 100 μm.

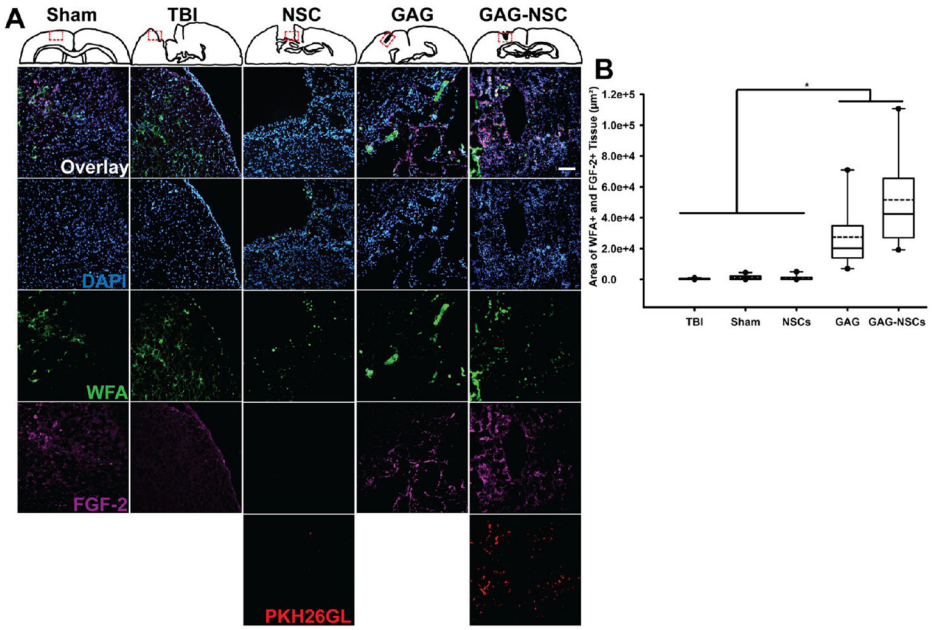

Figure 4.

FGF2 presence in brain tissue. (A) Representative images of the region corresponding to the red dotted box in coronal brain sections obtained from sham animals, and surrounding the lesion area in coronal brain sections obtained from TBI only, NSC only, CS-GAG only, and CS-GAG-NSC treated animals. Cellular nuclei are represented by DAPI (blue); CS-GAG and GalNAc presence is indicated by WFA labeling (green); and FGF2 labeling is indicated in magenta. Merged overlays are presented in the topmost panel. A significantly greater FGF2+ area was visualized in brain sections obtained from CS-GAG and CS-GAG-NSC treated animals when compared to sham and TBI only controls, and NSC only treated animals. Statistical significance is represented by '*', which indicates $p < 0.05$. Scale = 100 μm.

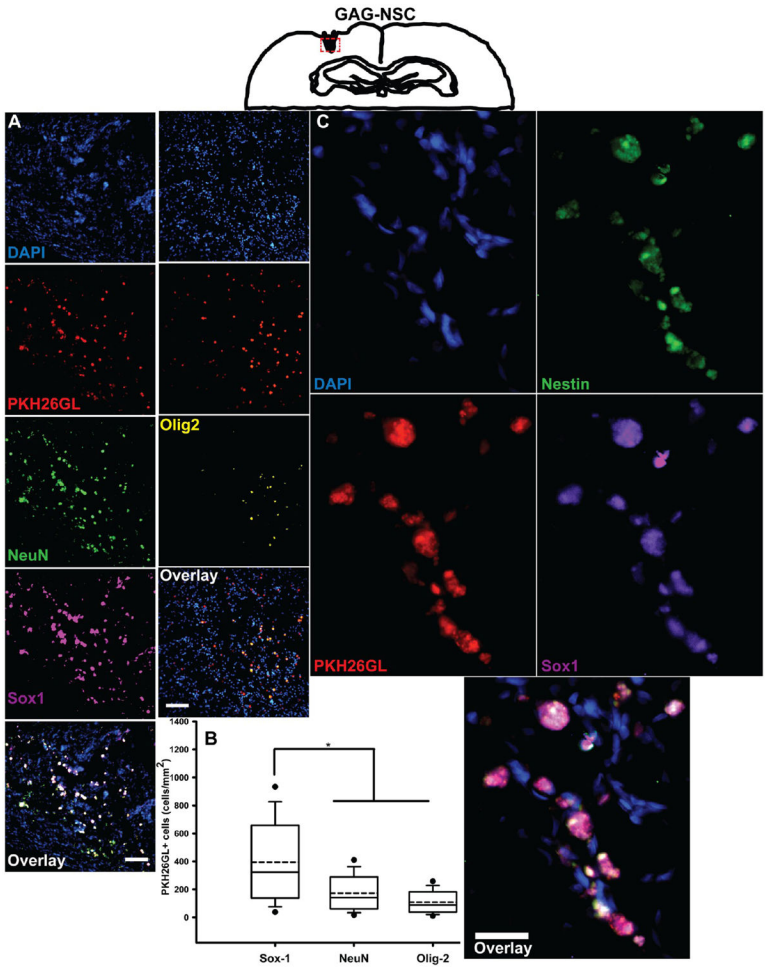

Figure 5.

Differentiation of NSCs transplanted in CS-GAG matrices. Representative images of the region corresponding to the red dotted box surrounding the lesion area in coronal brain sections obtained from CS-GAG-NSC treated animals. (A) Represents the neural cell differentiation of transplanted NSCs. Cellular nuclei are represented by DAPI (blue); transplanted NSCs are represented by PKH26GL labeled cells (red); NSCs differentiating into neurons are represented by NeuN labeling (green); NSC differentiating into oligodendrocytes are represented by the Olig2 label (yellow); undifferentiated NSCs are represented by the Sox1 label (magenta); Merged overlays are presented in the bottom most panels. Scale = 100 μm. (B) A significantly greater number of NSCs delivered in CS-GAG matrices maintained their undifferentiated state as demonstrated by the maintenance of Sox1 expression when compared to NSCs that differentiated into neurons or oligodendrocytes. Statistical significance is represented by '*', which indicates $p < 0.05$. (C) High-magnification images of PKH26GL$^+$ transplanted NSCs in the lesion site coexpressing the NSC markers Sox1 and nestin. Scale = 20 μm.

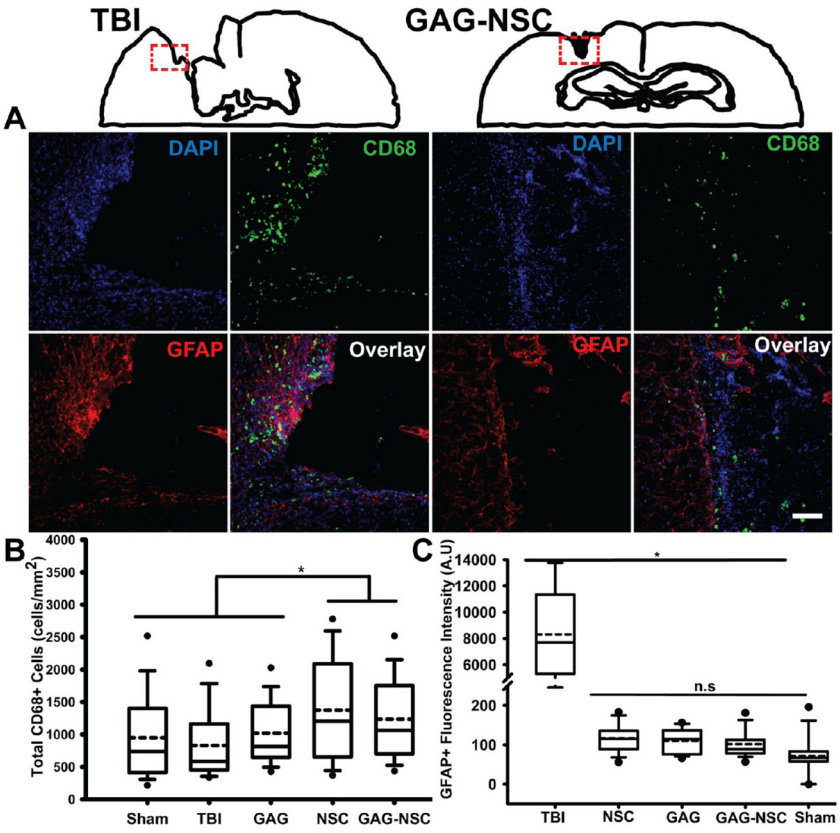

Figure 6.

Activated macrophage and reactive astrocyte presence surrounding the lesion site in TBI only control and CS-GAG-NSC treated animals. (A) Representative images of the region corresponding to the red dotted box surrounding the lesion area in coronal brain sections obtained from TBI only control, and CS-GAG-NSC treated animals. Cellular nuclei are represented by DAPI (blue); activated macrophages are represented by CD68 labeled cells (green); and reactive astrocytes are represented by GFAP labeled cells (red). Merged overlays are presented in the bottom right panels in each group. (B) A significantly greater CD68+ reactivity was observed in brain sections obtained from animals treated with NSCs only, and with CS-GAG-NSCs when compared to all other groups. (C) Brain tissue obtained from TBI only controls indicated a significantly increased GFAP immunoreactivity for reactive astrocytes when compared to all treatment groups and sham control. Statistical significance is represented by '*' which indicates $p < 0.05$. The lack of statistical significance between groups is denoted by 'n.s'. Scale =100 μm.

Table 1

List of Immunohistochemical Markers

target	antibody	vendor	dilutions	ref
neurons	NeuN	millipore	1:200	[21,23]
neurons	NF200	millipore	1:1000	[24]
astrocytes	GFAP	dako	1:1000	[19,22]
macrophages	CD68	AbD Serotec	1:500	[22]
NSCs	Sox1	1:200	1:200	[25]
NSCs	Nestin	Millipore	1:500	[19,20]
proliferating cells	Ki67	BD Biosciences	1:800	[26]
oligodendrocytes	Olig2	Millipore	1:250	[27]
fibroblast growth factor	FGF2	R&D Systems	1:200	[23]
N-acetylgalactosamine (GalNAc) residues linked to CS-GAGs	FITC -WFA	Vector Laboratories	50 μg/mL	[28]